

Design of Circular Array with Yagi-Uda Corner Reflector Antenna Elements and Camera Trap Image Collector Application

Suad Basbug*

Abstract—A six-element circular antenna array with Yagi-Uda corner reflector elements is proposed in order to achieve 360° beam-steering capability, high gain, and cost-effective design objectives. The array element is mainly composed by a Yagi-Uda antenna, a corner reflector, and a Wilkinson balun. For steering the main beam, instead of classical RF switching techniques, a virtual switching technique is offered. For this aim, each antenna element is connected to an affordable RF transceiver managed by a microcontroller. A USB hub is also used so that a computer operates all microcontrollers as peripheral devices. In this way, the switching operation can be performed in the software level. Furthermore, if every transceiver in the separate chain is set to a different frequency channel, a simultaneous communication is also possible with the help of the multithreading facility of the computer. In order to show the antenna array performance, the main antenna characteristics and test results are given. As a proof of concept, a wireless image collector scenario is also realized for a camera trap application. The results show that the circular antenna array design and switching technique work successfully.

1. INTRODUCTION

A dipole antenna is a very simple and effective solution for the wireless communications since it radiates equally in all directions in the azimuth plane. However, modern communication systems frequently need to concentrate the electromagnetic waves into certain directions in this plane, because the main beam steering and high directivity are often key factors for the long-distance communications and interference avoidance. Hence, the beam-steering antenna systems have attracted considerable attentions over the past decades.

During the design phase of an antenna system with 360° beam-steering capability, there are a few issues to be considered. Usually phased arrays are preferred since they are very capable of steering the main beam, but they may have to require complicated feeding networks [1]. Circular and concentric circular monopole antenna arrays are also used for beam-steering owing to their simple and effective structures. However, they generally radiate into the upper hemisphere. In case the radiation is also needed into the lower hemisphere, monopole antennas may not provide sufficient elevation coverage [2, 3]. The antenna array elements fixed on a surface or a direct course driven with phase shifters help to steer the main beam, but they generally scan up to range of $\pm 70^\circ$ [1, 4, 5]. For a full 360° scanning, pin diode switching [6, 7] or novel methods such as antenna systems with liquid metal parasitic elements [8] were also used. A compact profile for an antenna is mostly desired. Nonetheless, in general, there is a trade-off between the size of antenna system and gain [9–11].

In this paper, a circular antenna array with six Yagi-Uda corner reflector elements having 360° beam-steering capability is proposed. Other primary design objectives achieve a high gain, cost effective, and easy-to-produce antenna system. Yagi-Uda antenna is used for a high directivity. Corner reflector

Received 16 May 2020, Accepted 18 June 2020, Scheduled 5 July 2020

* Corresponding author: Suad Basbug (suadbasbug@gmail.com).

The author is with the Department of Electrical and Electronics Engineering, Nevsehir Haci Bektas Veli University, Nevsehir 50300, Turkey.

components are used for the same purpose and additionally to adjust the horizontal beamwidth to the intended angle in the design phase. Wilkinson balun maintains good return loss values. The six elements of the circular array are positioned every 60° around a ring on a hexagram-shaped chipboard to cover the whole azimuthal plane. Although the proposed array is capable to work with traditional phase shifters and RF switches for the same scanning purpose, a new technique is introduced with some additional advantages such as the possibility of synchronous communication. In this technique, the array elements are connected separately to transceivers controlled by microcontrollers. The single series of an antenna, transceiver, and microcontroller is hereafter referred to as the chain in this paper. A computer is in charge of managing the whole communication process, which has access to these microcontrollers in the chain via USB hub.

In order to test the proposed antenna array and virtual switching mechanism, a wireless data collection scenario is realized. In this scenario, the proposed antenna array system is used to collect photo images of wild animals taken automatically by camera traps with motion sensors. In the current situation, the wildlife scientists mostly collect the images manually from the camera traps [12]. The collecting methods built on wireless network sensors technologies inherently perform short distance communications, and eventually excessive number of wireless sensors that use multi-hop routing have to be employed for a wide coverage [13]. The mobile and satellite communication technologies are two other alternatives. However, it is well known that the mobile communication infrastructure may fall short of expected coverage, especially in unpopulated areas, and using satellite communication is an expensive choice for many applications [14].

2. 360° BEAM-STEERING CIRCULAR ANTENNA ARRAY

2.1. Array Element Design

The base structure of the array element of the proposed antenna array is shown in Fig. 1(a). The antenna is printed on an FR-4 substrate with 4.25 relative permittivity and 1.6 mm thickness. The antenna design starts with a traditional Wilkinson divider [15] to form the first part of a Wilkinson balun. The Wilkinson balun is chosen to have a good return loss [16]. The width of microstrip lines is chosen as 3.15 mm for 50Ω characteristic impedance. The width of 70.71Ω microstrip quarter wave lines used in the equal-split power divider is determined as 1.66 mm. After the divider, one of the output ports of the divider is lengthened by half wavelength on microstrip ($\lambda_g/2$) to provide a 180° phase shift before the dipole antenna to construct a balun. In order to avoid the negative effects of the sharp edges, the phase shifter microstrip branch is bent into two quarter circles and one semicircle with the help of three circles to maintain a smooth transition. The centers of circles A, B, and C in Fig. 1(a) are collinear. The radii of the circles are calculated to ensure that the centerline length of curved line is $\lambda_g/2$ longer than the straight line. The following equation is used to calculate the radius of circle B (r_b):

$$r_b = \frac{\lambda_g}{4(\pi - 2)} \quad (1)$$

Circles A and C have the same radius lengths, which are 3.15 mm shorter than the that of circle B. Two balanced parallel stripes are connected to the dipole antenna to feed it. Two strip lines as auxiliary reflectors take places just behind the dipole antenna. The lengths and locations of the dipole branches are determined by the parametric sweep feature of COMSOL Multiphysics simulation software [17]. The parametric sweep iterations reveal that if the distance between the dipole antenna and the reflector strip lines is longer than the current length, the directivity of the antenna decreases. On the other hand, if this distance is shortened, then the input impedance of antenna is changed dramatically. As a conclusion, it can be said that the current position of the dipole along the y -axis is optimum for this geometry. Fig. 1(b) shows the final form of the antenna element after adding four directors of Yagi-Uda part and two corner reflector plates. The directors and reflectors are fixed with the help of the polylactic acid holders manufactured by a simple 3D printer. The directors are wires with radius of 1.5 mm and length of 41 mm separated each other by a distance of 25 mm whereas the first director element is 20 mm from the substrate. The corner reflector plates are copper clad single-sided FR4 substrates with thickness of 1.6 mm and dimensions of 100×100 mm. The nearest edges of both reflector plates are

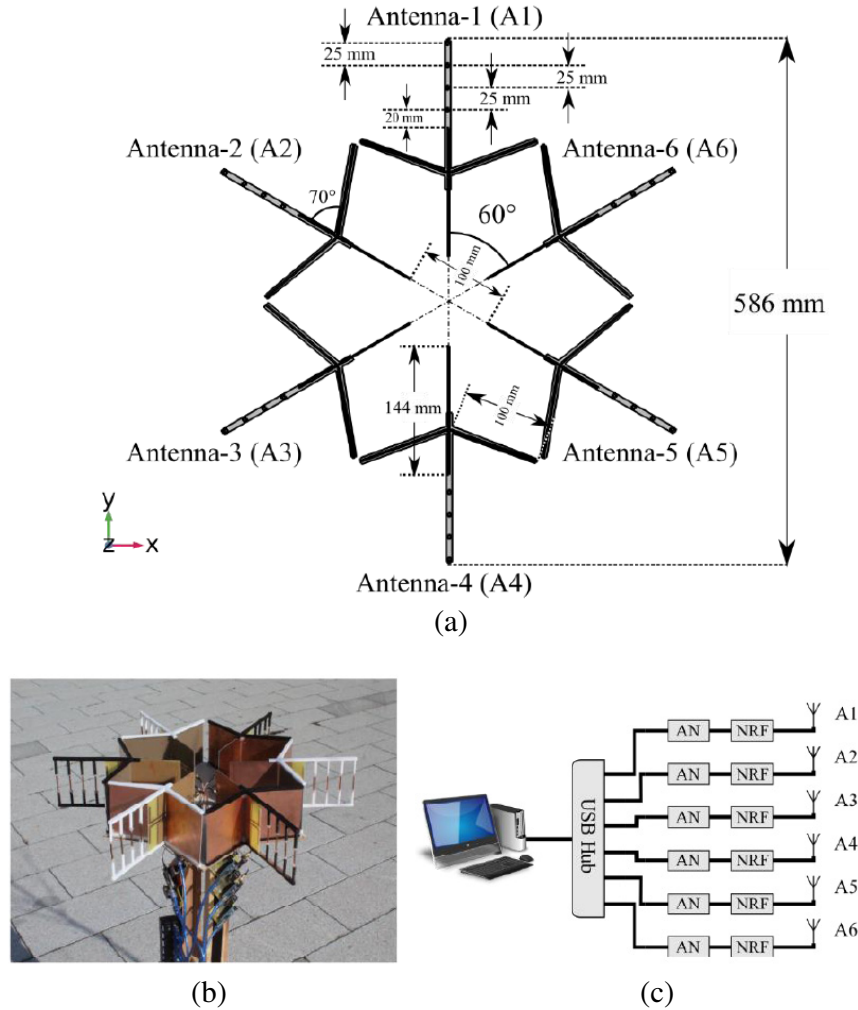


Figure 2. (a) Layout and dimensions of the proposed circular antenna array. (b) Manufactured circular antenna array and virtual switching equipment. (c) Switching mechanism diagram and transceiver chains of the array elements connected to the computer via USB hub.

and NRF. A multiport USB hub is used to connect six ANs to a computer which owns a program written in Java language. The computer program is capable to manage the communication and performs the virtual switching by activating/deactivating each chain consisting of an AN, NRF, and one of the array elements. Naturally, the proposed switching method is not as fast as the other alternatives such as solid state or micro electro mechanic switches. But it can be very useful for the applications which do not need to be agile. Additionally, in this technique, if the transceiver chains set to different frequency channels in 2.4-2.5 GHz range, the communications with the remote nodes can be done via different channels simultaneously.

2.3. Image Collector System Scenario and Application

The main idea in the image collector system scenario is wirelessly fetching wild animal photo images taken by the camera traps scattered over the terrain. The system consists of two main parts. The first one is the proposed antenna array and its control mechanism as an image collector. The second one is a transmitter that emulates a camera trap. The transmitter is composed of one instance of the proposed array element as a directive antenna, an NRF, an Arduino Mega (AMG) microcontroller, and an SD card which contains image files. When both ends are ready, AMG starts reading the image file from the SD card byte-by-byte and sends them in the 32-byte NRF packet formats to the image collector which

utilizes the proposed antenna array. At the end of the file transmission process, the collector checks the received data by considering the length of the file to determine the lost packets. It makes a lost packet lists and sends it to the transmitter. The transmitter starts again the transmission process, but this time only packets which are in the lost packets list are sent. This last procedure is repeated until there is not any unreceived packet in the receiver side. Then, the collector saves the received data into a file with a time stamp name. Lastly, collector system also creates a log file which includes the key transactions and total transmission time.

3. MEASUREMENT AND TEST RESULTS

3.1. Antenna Array Characteristics

The $|S_{11}|$ measurements are carried out by using miniVNA Tiny that has a frequency range between 1 MHz and 3 GHz. The radiation pattern is achieved by using ADF4351 signal generator and AD8318 logarithmic detector in the open-air [22]. For the pattern measurement, the antenna under test connected to the logarithmic detector is set on a turntable controlled by a stepper motor. The signal generator continuously radiates electromagnetic waves at 2.45 GHz through a horn antenna. Measurement is started remotely by means of a computer that connects to the microcontroller which drives the stepper motor. The remote control is carried out with a Bluetooth connection. Once the measurement starts, the Bluetooth module connected to the microcontroller stops the communication with the computer to avoid any possible interference. The measurement is performed on the horizontal plane. All simulations are performed by using COMSOL Multiphysics with RF Module [17].

The simulated and measured $|S_{11}|$ parameter results of the antenna array elements are shown in Fig. 3. The results are different from each other more or less owing to imperfect fabrication processes of the array elements. But they are all in good agreement with the simulated $|S_{11}|$ result in terms of the main criteria. For example, all measured $|S_{11}|$ values are lower than -10 dB within 2.4–2.5 GHz. Even the highest value of the worst result, which belongs to A6, is below -13.66 dB. A4 owns the best $|S_{11}|$ result that is -37 dB.

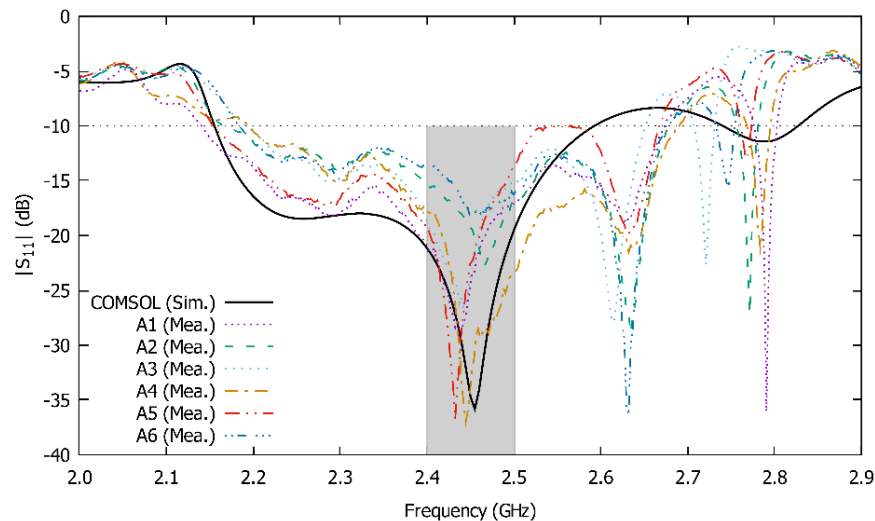


Figure 3. Simulated and measured $|S_{11}|$ parameter values of the antenna array elements.

Figure 4(a) shows the simulated and measured radiation patterns at 2.45 GHz center frequency. All values are normalized to their maximums. From Fig. 4(a), it can be said that the measured radiation pattern is in good agreement with the simulated one. The slight difference between the measured and simulated results might be due to imperfect fabrication and measurement conditions. It can also be deduced that from the -3 dB ring in Fig. 4(a) the circular array can cover the whole azimuth plane by means of the proper beamwidth of the array elements. For further investigation, the simulated radiation

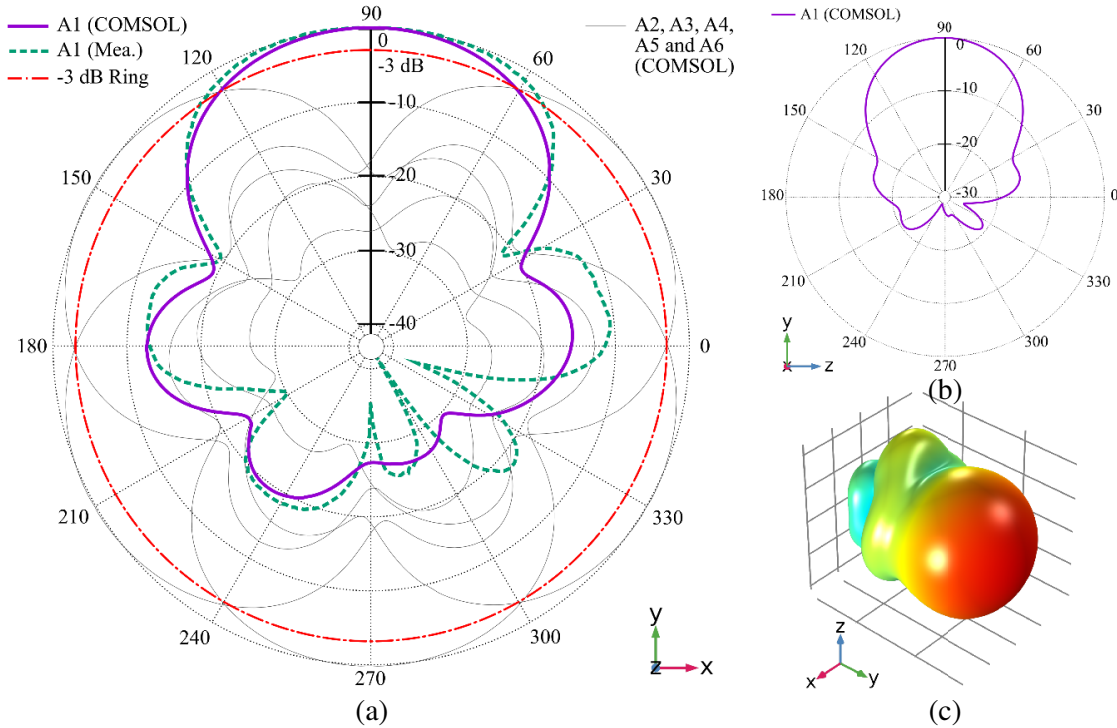


Figure 4. (a) Simulated and measured radiation patterns of the antenna array elements at 2.45 GHz on xy -plane. (b) Simulated radiation pattern of a single array element at 2.45 GHz on yz -plane. (c) Simulated 3D radiation pattern of a single array element at 2.45 GHz.

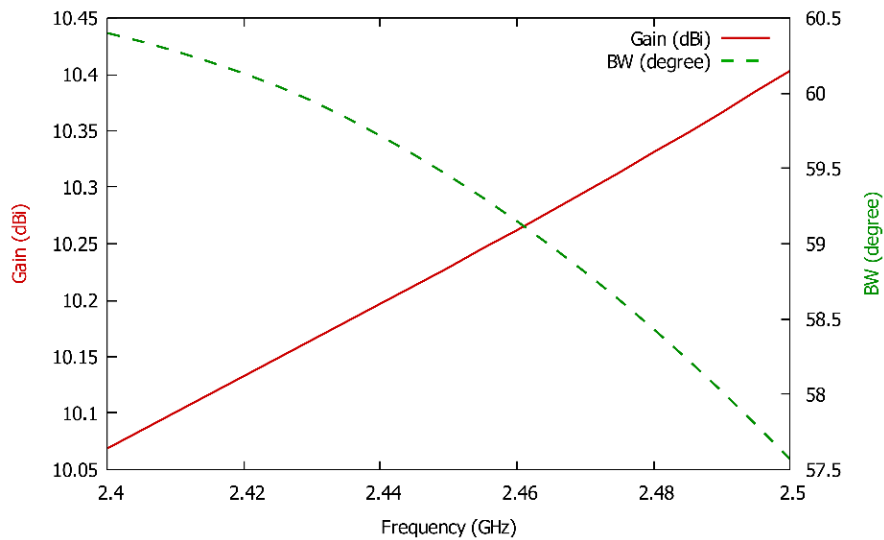


Figure 5. Simulated gain and half-power beamwidth (BW) variations of a single element of the proposed antenna array from 2.4 GHz to 2.5 GHz.

pattern of a single array element at 2.45 GHz on yz -plane given Fig. 4(b) can be used. Additionally, Fig. 4(c) presents a simulated 3D radiation pattern of a single array element at 2.45 GHz.

In Fig. 5, the simulated gain and half-power beamwidth changes of the array element over the frequency range 2.4–2.5 GHz are shown. It is clear that the gain and beamwidth deviations in the intended frequency range are very small.

3.2. Simultaneous Communication Test

When the six different transceiver chains are set to different frequency channels within the frequency range 2.4–2.5 GHz, the chains can carry out the communication with the other nodes simultaneously. In order to validate this assertion and determine the necessary frequency bandwidth for a proper simultaneous communication, a small test environment is established. There are three units, namely a transmitter, a receiver, and a jammer in this test environment. The transmitter and receiver have the same configurations with the transmitter and image collector system explained in Section 2, respectively. Both of them are also set to 2463 MHz frequency. The jammer is mainly composed of an ADF4351 signal generator and a directive horn antenna. Three units are separated from each other by 1.5 meters as forming an equilateral triangle. The jammer radiates its sinusoidal signal by scanning the 2.4–2.5 GHz frequency range with the help of a microcontroller unit while the transmitter sends the packets filled with random values, and the receiver catches them. The receiver displays the average received packets per second on a display. Fig. 6 shows the resultant plot. From Fig. 6, it can be concluded that for a safe simultaneous communication, 6 MHz bandwidth should be dedicated to each single channel whereas the datasheet of NRF [21] states that a channel occupies a bandwidth of 2 MHz at 2 Mbps. Under our test conditions, the receiver is still affected by the jammer at 2461 MHz and 2465 MHz; consequently, the numbers of the received packets are not at the ideal level in this range.

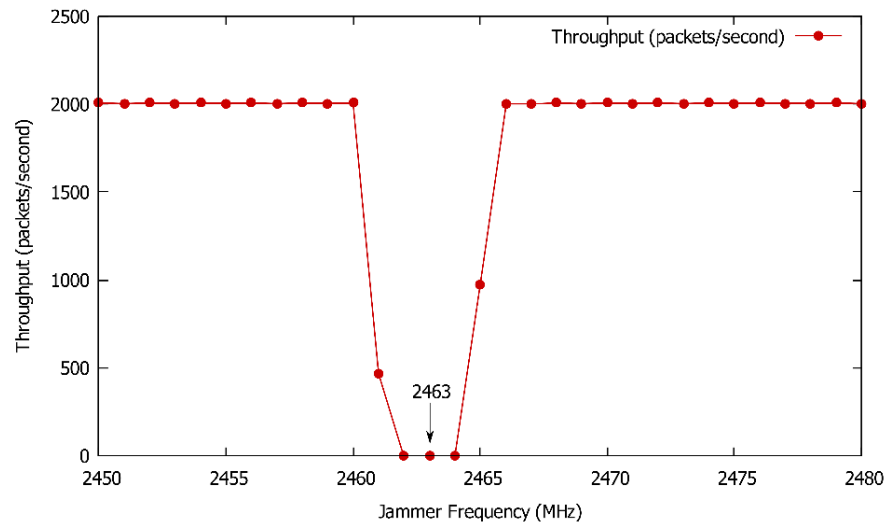


Figure 6. Received packets per second under 2463 MHz jamming condition.

3.3. Image Collector Application Results

The system has been configured for a transmission of an HD quality leopard image file in JPEG format. The dimensions of the image file are 1920×1080 pixels, and its file size is 501 KB. The circular antenna array with the image collector system was mounted on the rooftop of a building next to Nevsehir Haci Bektas Veli University campus. After activating the collector system, the transmitter unit as the camera trap emulator was moved to different far distances around the region. The locations where the transmitter was triggered had been chosen by means of an online visualization software that can create the line-of-sight profile between a source and a target on the map [23]. Fig. 7 shows the distances between the transmitter and image collector for different successful transmission cases. There are also the time spent values of these transmissions. In the experiment, the transmission of the image file lasts 63 seconds for the farthest distance (Deller) that is 21 km. The same image file is transmitted from the nearest point (Sulusaray), which is 5.5 km, to the collector within 16 seconds. In order to evaluate these values properly, it is worthwhile to mention that the total transmission time is 13 seconds if there is not any lost packet. In general, longer distance communications need the more time to complete the whole

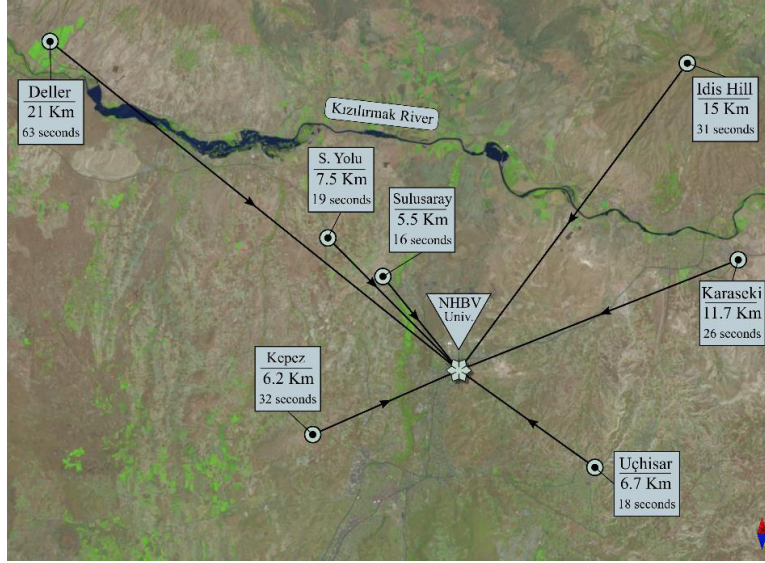


Figure 7. Distances between the transmitters and receiver (image collector) and elapsed times for the transmission of the image file.

file transmission. This situation is an expected consequence since path loss is an inevitable attenuation type which highly depends on the distance in the analysis of the link budget of a wireless communication system. Eventually, the number of lost packets that need to be resent increases because weaker signals are more easily disturbed by any kind of noises. But the transmission from the transmitter in Kepez to the receiver in the campus takes longer time than those of the farther cases except Deller. This unusual result can be explained with the Fresnel zone effect. The Kepez communication example had a line-of-sight between the transmitter and receiver as the other examples. However, there are a lot of obstacles near the direct-path contrary to the other cases which have clearer line-of-sights. These obstacles are causatives of the deflected-path waves which may lead to destructive interference. The overall results of the experiment show that the proposed antenna array system works successfully.

4. CONCLUSION

In this paper, the design of a six-element circular antenna array having high gain and 360° beam steering capability is introduced. The main parts of the array elements are a Yagi-Uda antenna, a corner reflector, and a Wilkinson balun. Additionally, in order to aim the main beam of the antenna system to desired directions, a virtual switching is proposed. In this switching technique, each chain has its own transceiver and microcontroller units. A computer manages these chains via USB hub. The main characteristics of the antenna are given. The $|S_{11}|$, gain, and beamwidth values over the frequency range 2.4–2.5 GHz are very good. The beam-steering and simultaneous communication can be achieved by the proposed virtual switching method. A wireless image collector scenario for wildlife camera traps is performed. The results show that the proposed antenna and switching system work successfully for the desired aim.

REFERENCES

1. Labadie, N. R., S. K. Sharma, and G. M. Rebeiz, "A novel approach to beam steering using arrays composed of multiple unique radiating modes," *IEEE Trans. Antennas Propag.*, Vol. 63, No. 7, 2932–2945, Jul. 2015.
2. Scott, H. and V. F. Fusco, "360° electronically controlled beam scan array," *IEEE Trans. Antennas Propag.*, Vol. 52, No. 1, 333–335, Jan. 2004.

3. Sibille, A., C. Roblin, and G. Poncelet, "Circular switched monopole array for beam steering wireless communication," *Electron. Lett.*, Vol. 33, No. 7, 551–552, Mar. 1997.
4. Debogović, T. and J. Perruisseau-Carrier, "Array-fed partially reflective surface antenna with independent scanning and beamwidth dynamic control," *IEEE Trans. Antennas Propag.*, Vol. 62, No. 1, 446–449, Jan. 2014.
5. Ji, L., G. Fu, and S.-X. Gong, "Array-fed beam-scanning partially reflective surface (PRS) antenna," *Progress In Electromagnetics Research Letters*, Vol. 58, 73–79, 2016.
6. Lai, M. I., T. Y. Wu, J. C. Hsieh, C. H. Wang, and S. K. Jeng, "Compact switched-beam antenna employing a four-element slot antenna array for digital home applications," *IEEE Trans. Antennas Propag.*, Vol. 56, No. 9, 2929–2936, Sep. 2008.
7. Wounchoum, P., D. Worasawate, C. Phongcharoenpanich, and M. Krairiksh, "A switched-beam antenna using circumferential-slots on a concentric sectoral cylindrical cavity excited by coupling slots," *Progress In Electromagnetics Research*, Vol. 120, 127–141, 2011.
8. Rodrigo, D., L. Jofre, and B. A. Cetiner, "Circular beam-steering reconfigurable antenna with liquid metal parasitics," *IEEE Trans. Antennas Propag.*, Vol. 60, No. 4, 1796–1802, Apr. 2012.
9. Alam, M. S., Y. Wang, N. Nguyen-Trong, and A. Abbosh, "Compact circular reconfigurable antenna for high directivity and 360° beam scanning," *IEEE Antennas Wireless Propag. Lett.*, Vol. 17, No. 8, 1492–1496, Aug. 2018.
10. Ge, L., K. M. Luk, and S. Chen, "360° beam-steering reconfigurable wideband substrate integrated waveguide horn antenna," *IEEE Trans. Antennas Propag.*, Vol. 64, No. 12, 5005–5011, 2016.
11. Yang, Y. and X. Zhu, "A wideband reconfigurable antenna with 360° beam steering for 802.11ac WLAN applications," *IEEE Trans. Antennas Propag.*, Vol. 66, No. 2, 600–608, Feb. 2018.
12. Kays, R., B. Kranstauber, P. Jansen, C. Carbone, M. Rowcliffe, T. Fountain, and S. Tilak, "Camera traps as sensor networks for monitoring animal communities," *Proc. 34th IEEE Conf. Local Computer Network*, 811–818, Zurich, Switzerland, Oct. 2009.
13. Camacho, L., R. Baquerizo, J. Palomino, and M. Zarzosa, "Deployment of a set of camera trap networks for wildlife inventory in western amazon rainforest," *IEEE Sensors J.*, Vol. 17, No. 23, 8000–8007, Dec. 2017.
14. Bagree, R., V. R. Jain, A. Kumar, and P. Ranjan, "TigerCENCE: Wireless image sensor network to monitor tiger movement," *Real-World Wireless Sensor Networks*, 13–24, Springer, Berlin, Heidelberg, 2010.
15. Pozar, D. M., *Microwave Engineering*, 3rd Edition, Wiley, Hoboken, NJ, USA, 2004.
16. Antoniadou, M. A. and G. V. Eleftheriades, "A broadband Wilkinson balun using microstrip metamaterial lines," *IEEE Antennas Wireless Propag. Lett.*, Vol. 4, 209–212, 2005.
17. COMSOL Multiphysics RF Module v. 5.4. COMSOL AB, Stockholm, Sweden, [online], available: <https://www.comsol.com/rf-module>, accessed on: May 16, 2020.
18. Kraus, J. D., "The corner-reflector antenna," *Proc. Inst. Radio Eng.*, Vol. 28, No. 11, 513–519, Nov. 1940.
19. Sterr, U. O., A. D. Olver, and P. J. B. Clarricoats, "Variable beamwidth corner reflector antenna," *Electron. Lett.*, Vol. 34, No. 11, 1050–1051, May 1998.
20. Milijić, M., A. D. Nešić, and B. Milovanović, "Design, realization, and measurements of a corner reflector printed antenna array with cosecant squared-shaped beam pattern," *IEEE Antennas Wireless Propag. Lett.*, Vol. 15, 421–424, 2016.
21. Nordic Semiconductors, "Single chip 2.4 GHz transceiver," nRF24L01+ datasheet, Sep. 2008.
22. Emin, B. and S. Basbug, "A low cost measurement system for antenna radiation patterns with logarithmic RF detector," *Proc. International Turkic World Congress on Science and Engineering*, 800–808, Nigde, Turkey, Jun. 17–18, 2019.
23. Line-of-sight and path profiler software, [online], available: <http://heywhatsthat.com/>, accessed on: May 16, 2020.